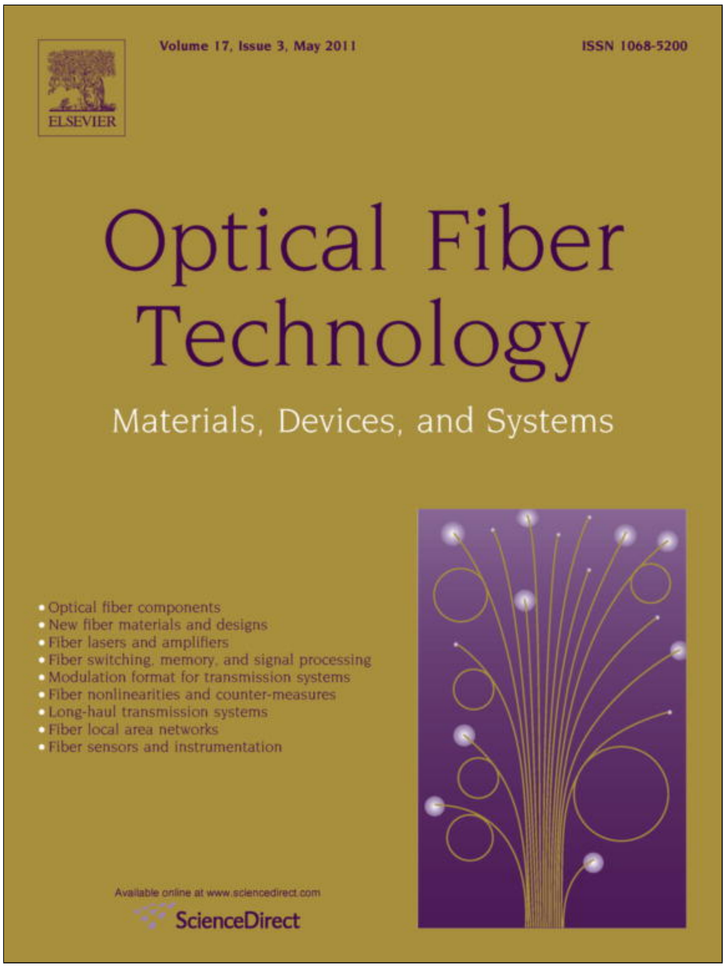
Volume 17, Issue 3, May 2011
ISSN 1068-5200
ELSEVIER
Optical Fiber Technology
Materials, Devices, and Systems
• Optical fiber components
• New fiber materials and designs
• Fiber lasers and amplifiers
• Fiber switching, memory, and signal processing
• Modulation format for transmission systems
• Fiber nonlinearities and counter-measures
• Long-haul transmission systems
• Fiber local area networks
• Fiber sensors and instrumentation
Available online at www.sciencedirect.com
ScienceDirect

Optical Fiber Technology 17 (2011) 191–195

Contents lists available at ScienceDirect

Optical Fiber Technology

www.elsevier.com/locate/yofte

A wavelength selective bidirectional isolator for access optical networks

Xi-kui Hu [a], Zhang-di Huang [a], Su-shan Li [a], Fei Xu [a], Beckham Chen [b], Yan-qing Lu [a,b,*]

[a] College of Engineering and Applied Sciences and National Laboratory of Solid State Microstructures, Nanjing University, Nanjing 210093, China
[b] Light Master Technology Inc., Ningbo 315806, China

ARTICLE INFO

Article history:
Received 22 October 2010
Revised 1 February 2011
Available online 12 March 2011

Keywords:
Optical isolator
Magneto-optical effect
Jones Matrix
Optical communications

ABSTRACT

A wavelength selective bidirectional optical isolator is proposed. Being different from conventional isolators, a well-designed wave plate is employed and works together with the Faraday rotator. Different wavelengths thus experience different phase retardation so that wavelength-dependent polarization states are obtained for bidirectional beams. As an example, a (1.49 μm, 1.31 μm) wavelength selective isolator is proposed, which means only 1.49 μm light can propagate along one-direction while the opposite wave is just for 1.31 μm light. Over 60 dB optical isolation is obtained by selecting suitable wave plate thickness and orientation. This interesting isolator may have promising applications in access optical networks.

1. Introduction

Breaking the reciprocity of light can lead to an important class of optical devices such as isolators, which are widely used to protect the semiconductor laser devices from the unwanted reflected light. Isolators are indispensable for the development of optical devices, especially in optical communication system, for example, in Passive Optical Networks (PONs) [1–4]. PON is probably the first Fiber to the *x* (FTT*x*) technology, in which unidirection plays an important role [5]. So, there are many works about isolators. Although some new nonlinear optics based isolators have been proposed, the magneto-optical (MO) isolator is still the only one being practically used [6,7]. Generally, conventional MO isolators only work at a single-wavelength. However, with the expansion of information, multi-wavelengths are employed in the optical signals [8]. For example, the G.983.3 standard specifies wavelength division duplex on a single fiber with the 1.31 μm wavelength window for upstream transmission and the 1.49 μm wavelength window for downstream. The recent IEEE802.3av standard regulates more complicated wavelength allocation for upstream and downstream lights. In order to protect the network well, a bidirectional wavelength selective in-line isolator would be attractive to define the wavelength-dependent propagations, which means only the light with specific wavelength and preset direction could travel in the network. We believe this is important in access PONs and also might be useful for other fiber-optic communication or sensing applications.

In this work, we proposed the design principle of a wavelength selective bidirectional isolator for dual-wavelength. Being different from the commercially available MO isolator, an extra wave plate is employed with well-designed phase retardation and orientation. A (1.49 μm, 1.31 μm) bidirectional isolator is thus obtained with promising applications in PONs. Although a bidirectional isolator has been reported before in DWDM network [9], the discrete and far-separated working wavelengths in PONs result in more difficulty in realizing bidirectional isolation. It is necessary to study the design and optimization of such an isolator in fast growing access networks.

2. Bidirectional isolator

Fig. 1 depicts the schematic diagram of a bidirectional isolator. It is still similar to the conventional MO isolator with a Faraday rotator. Differently, an additional specially-designed wave plate is sandwiched between the Faraday rotator and the polarizer [10–12]. Normally the wave plate is a fixed birefringent crystal, but it also could be a homogeneous alignment liquid crystal (LC) cell with tunable capability [13]. Due to the wavelength dependency, it can act as a full wave plate for one wavelength (λ_1) while be a half wave plate for another wavelength (λ_2). Hence, compared with a commercially used MO isolator, the polarization of λ_1 light is unaffected. If the polarizer and analyzer have a 45° angle separation and the Faraday rotator changes the light polarization for the same angle, λ_1 light thus may propagate from left to right freely as shown in Fig. 1. When it bounces back, the λ_1 light passes through the Faraday rotator with its polarization orthogonal to the left polarizer because of the MO non-reciprocity. In this case, the light is blocked at the left polarizer just like a normal isolator.

* Corresponding author at: College of Engineering and Applied Sciences and National Laboratory of Solid State Microstructures, Nanjing University, Nanjing 210093, China. Fax: +86 83595535.
E-mail address: yqlu@nju.edu.cn (Y.-q. Lu).

1068-5200/$ - see front matter © 2011 Elsevier Inc. All rights reserved.
doi:10.1016/j.yofte.2011.02.009

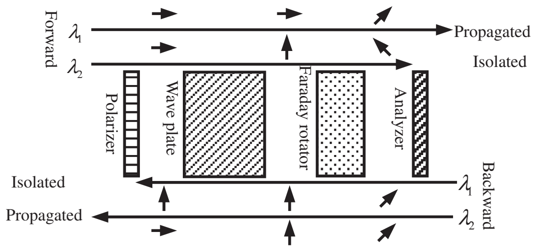

Fig. 1. Schematic of a bidirectional isolator with wavelength selective function.

However, for λ_2 light, the combination of left polarizer and the half wave plate is just like a 90° rotated "polarizer" if the wave plate's optical axis is 45°-orientated. In this situation, the λ_2 light is isolated from left to right, while the opposite propagation is allowed for λ_2 light with low loss. A wavelength selective isolator is thus obtained.

Although the principle of a bidirectional isolator looks clear, the detailed design is still not so straightforward because the polarization rotation of the Faraday rotator varies with different wavelengths. Therefore the optical axis and thickness of the wave plate should be carefully designed as well as the angle between the polarizer and analyzer to optimize the transmittances and isolations.

Fig. 2 shows the polarization evolution of λ_1 and λ_2 lights for both forward and backward propagation respectively. With no loss of generality, we define that z-axis is the propagation direction and x is the transmission axis of left polarizer. α describes the wave plate's optical axis orientation angle with respect to x-axis. The angle between polarizer and analyzer is ϕ. g_1 and g_2 are the Faraday rotation angles for λ_1 and λ_2 respectively. Fig. 2a and b denotes the

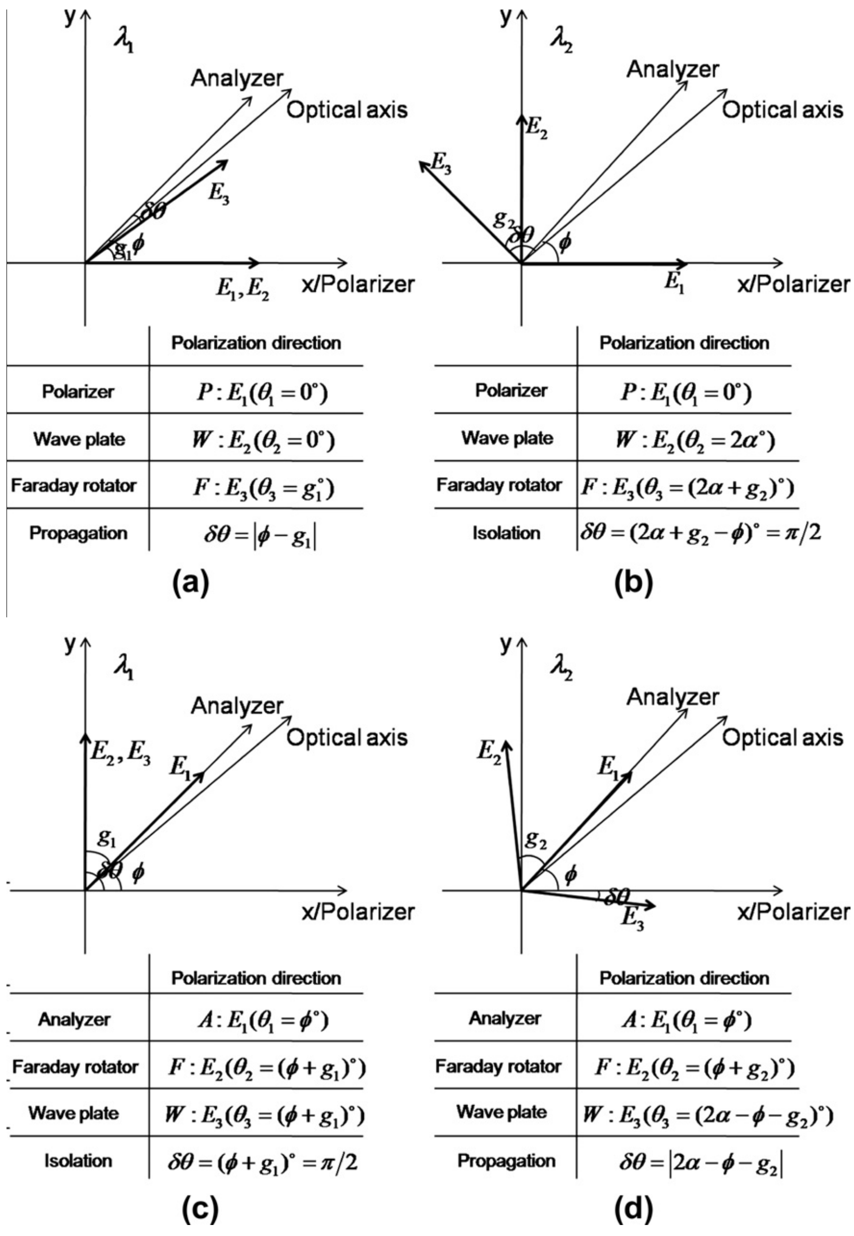

Fig. 2. Polarization evolution of the bidirectional isolator. A polarizer is placed along x-axis while the analyzer forms a ϕ angle with respect to the polarizer. α represents the wave plate's orientation angle. g_1 and g_2, are the Faraday rotation angles for λ_1 and λ_2 that are marked in the figure. θ_1, θ_2 and θ_3 correspond to the angles between x-axis and the light polarization direction, $\boldsymbol{E}_1$, $\boldsymbol{E}_2$ and $\boldsymbol{E}_3$, respectively. (a) and (b) are for the forward lights, while (c) and (d) represent the backward lights. The corresponding wavelengths are marked in the figure.

forward propagation condition. $\boldsymbol{E}_1$, $\boldsymbol{E}_2$ and $\boldsymbol{E}_3$ represent the light polarization direction changes after passing through the polarizer, wave plate and Faraday rotator respectively. θ_1, θ_2 and θ_3 correspond to the angles between $\boldsymbol{E}_{1,2,3}$ and *x*-axis. Then, $\delta\theta$ is the angle between the output signal polarization direction and the transmission axis of analyzer. Thus, $\cos^2(\delta\theta)$ can express the transmittance. As the wavelength dependence of wave plate, it can act as a full wave plate for λ_1 light. Therefore, its polarization is unaffected. As shown in Fig. 2a, $\theta_1 = \theta_2$, that is to say, $\boldsymbol{E}_1$ and $\boldsymbol{E}_2$ have the same polarization directions. However, in Fig. 2b, it is a half wave plate for λ_2 light, leading to different polarization directions of $\boldsymbol{E}_1$ and $\boldsymbol{E}_2$. Therefore, $\delta\theta$ will be different for λ_1 and λ_2. Scilicet, the transmissions are different for λ_1 and λ_2. When $\delta\theta = \pi/2$, namely the output light polarization is orthogonal to the analyzer, it is isolated as shown in Fig. 2b. Otherwise, light can propagate as shown in Fig. 2a. For the backward propagated light, $\boldsymbol{E}_1$, $\boldsymbol{E}_2$ and $\boldsymbol{E}_3$ represent the light fields after passing through the analyzer, Faraday rotator and wave plate respectively as shown in Fig. 2c and d. Similarly, θ_1, θ_2 and θ_3 correspond to their polarization directions. $\delta\theta$ is the angle between the output signal polarization direction and the transmission axis of polarizer. The status is reversed, λ_1 light is blocked and the λ_2 signal travels with low loss, corresponding to Fig. 2c and d respectively.

As analyzed above, for a wavelength selective bidirectional isolator, the λ_2 light is blocked in the forward direction, so that,

$$2\alpha + g_2 - \phi = \pi/2. \tag{1}$$

And the λ_1 light is blocked in the backward direction,

$$\phi + g_1 = \pi/2. \tag{2}$$

The phase retardation of wave plate is defined by,

$$\Gamma_{1,2} = 2\pi\Delta n l/\lambda_{1,2}, \tag{3}$$

where λ is the wavelength, Δn is birefringence and l is the wave plate thickness. Assume the lights incidence vertically to the isolator, the Jones Matrix method could be used to analyze the light transmission properties [14]. Without consideration of the Fresnel reflection in each surface, the transmittances of the output optical signals are,

$$\begin{aligned}
T^{(1)}_{forward} &= \cos^2(g_1 - \phi)\cos^2(\Gamma_1/2) + \cos^2(g_1 - \phi - 2\alpha)\sin^2(\Gamma_1/2),\\
T^{(2)}_{forward} &= \cos^2(g_2 - \phi)\cos^2(\Gamma_2/2) + \cos^2(g_2 - \phi - 2\alpha)\sin^2(\Gamma_2/2),\\
T^{(1)}_{backward} &= \cos^2(g_1 + \phi)\cos^2(\Gamma_1/2) + \cos^2(g_1 + \phi + 2\alpha)\sin^2(\Gamma_1/2),\\
T^{(2)}_{backward} &= \cos^2(g_2 + \phi)\cos^2(\Gamma_2/2) + \cos^2(g_2 + \phi + 2\alpha)\sin^2(\Gamma_2/2).
\end{aligned} \tag{4}$$

The superscripts (1) and (2) represent λ_1 and λ_2, respectively. Γ_1 and Γ_2 are the phase retardation of the wave plate for λ_1 and λ_2. For full wave plate, $\Gamma = 2m\pi$, and for half wave plate, $\Gamma = (2n + 1)\pi$. Both m and n are integers.

Usually the dielectric permittivity tensor of the Faraday rotator can be written as,

$$\varepsilon = \begin{pmatrix} \varepsilon & 0 & 0 \\ 0 & \varepsilon & i\varepsilon' \\ 0 & -i\varepsilon' & \varepsilon \end{pmatrix}. \tag{5}$$

The off-diagonal element ε', which originates from a first-order magneto-optic effect, is related to the Faraday rotation Θ_F by,

$$\varepsilon' = 2n\Theta_F/k_0. \tag{6}$$

Here, $n = \sqrt{\varepsilon}$ is the refractive index of the material, and k_0 is the wave-number in vacuum. That is to say, the rotation angle g of the Faraday rotator is inversely proportion to wavelength,

$$g_{1,2} \propto C/\lambda_{1,2}. \tag{7}$$

C is a constant of the Faraday rotator [15]. In our design, the target wavelengths of the optical signals are (λ_1, λ_2) = (1.49 μm, 1.31 μm), which are typical wavelengths in access optical networks. At an optimized condition, namely the forward and backward lights have the same transmittance for λ_1 and λ_2, i.e.,

$$|\phi - g_1| = |2\alpha - \phi - g_2|. \tag{8}$$

As a consequence, the isolator parameters could be solved from Eqs. (1), (2), (7), and (8) obtained above.

The constant $C = 40.48°$ for $\lambda = 1.55$ μm, that is to say, the Faraday rotation angles are $g_1 = 42.11°$ for $\lambda_1 = 1.49$ μm and $g_2 = 47.89°$ for $\lambda_2 = 1.31$ μm, respectively. Place the wave plate's optical axis $\alpha = 45°$, and the angle between polarizer and analyzer is set as $\phi = 47.89°$. Then $\delta\theta = 5.78°$ is obtained for both λ_1 in the forward direction and λ_2 in the backward as shown in Fig. 2a and d, respectively. The transmittances of the output optical signals can be simplified,

$$\begin{aligned}
T^{(1)}_{forward} &= \cos^2(\delta\theta)\cos^2(\Gamma_1/2) + \sin^2(\delta\theta)\sin^2(\Gamma_1/2),\\
T^{(2)}_{forward} &= \cos^2(\Gamma_2/2),\\
T^{(1)}_{backward} &= \sin^2(\Gamma_1/2),\\
T^{(2)}_{backward} &= \sin^2(\delta\theta)\cos^2(\Gamma_2/2) + \cos^2(\delta\theta)\sin^2(\Gamma_2/2).
\end{aligned} \tag{9}$$

From Eq. (9), when $\Gamma_1 = 2m\pi$ (m is an integer),

$$\begin{aligned} T^{(1)}_{forward} &= \cos^2(\delta\theta) \\ T^{(1)}_{backward} &= 0 \end{aligned}. \tag{10}$$

Similarly, when $\Gamma_2 = (2n + 1)\pi$ (n is an integer),

$$\begin{aligned} T^{(2)}_{forward} &= 0 \\ T^{(2)}_{backward} &= \cos^2(\delta\theta) \end{aligned}. \tag{11}$$

That is to say, if the wave plate is full wave for λ_1 while it is half wave for λ_2, a bidirectional isolator will be achieved. Meanwhile, the related transmittances are determined by $\delta\theta$. If the parameters are set inappropriate, $\delta\theta$ will be much larger, leading to remarkable insertion loss.

Assume that the wave plate is made of Quartz crystal with birefringence index $\Delta n = 0.00846$, the crystal thickness thus should satisfy,

$$\begin{aligned} \Gamma_1 &= \tfrac{2\pi\Delta n l}{\lambda_1} = 2m\pi \\ \Gamma_2 &= \tfrac{2\pi\Delta n l}{\lambda_2} = (2n+1)\pi \end{aligned}. \tag{12}$$

Here both m and n are integers. If the material index of wave plate depends on wavelength, Δn is no longer a constant. Eq. (12) will be instead of,

$$\begin{aligned} \Gamma_1 &= \tfrac{2\pi\Delta n_1 l}{\lambda_1} = 2m\pi \\ \Gamma_2 &= \tfrac{2\pi\Delta n_2 l}{\lambda_2} = (2n+1)\pi \end{aligned}. \tag{13}$$

Δn_1 and Δn_2 are the birefringence index of wave plate for λ_1 and λ_2 separately, which are normally different. The obtained wave plate thickness changes accordingly. The corresponding working wavelengths thus have a slight offset as well, which could be solved by system calibration. To totally overcome this problem, two wave plates with opposite temperature coefficients could be employed and bonded together so that the net effect of wave plate becomes wavelength insensitive. However, normally this requirement (Eq. (12)) is too strict to be satisfied. The isolation for one-direction could be very high while the performances along the opposite way may be much worse. Therefore, we have to optimize the wave plate thickness to obtain large optical isolations for λ_1 and λ_2 at the same time. Fig. 3 shows the isolator's transmittances at different Quartz thicknesses. In the forward direction, the solid

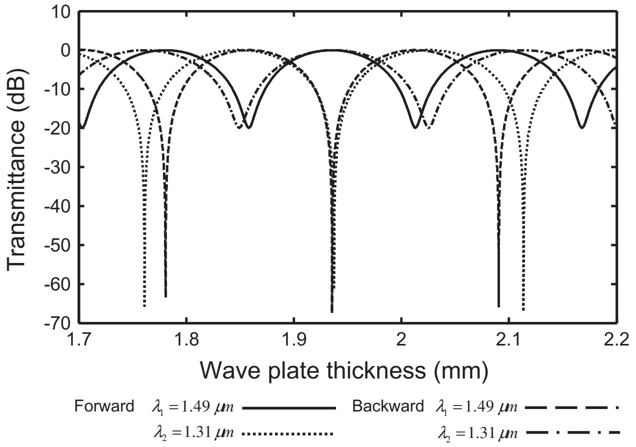

Fig. 3. Forward and backward transmittances as a function of the wave plate thicknesses. High transmissions and great isolations for both (λ_1) and (λ_2) lights are be obtained simultaneously at the wave plate thickness of 1.936 mm.

and dotted lines represent the λ_1 and λ_2 light respectively. In the backward direction, the dashed and dash-dotted lines represent the λ_1 and λ_2 light respectively. To meet the working wavelengths (1.49 μm, 1.31 μm), the optimized Quartz crystal thickness is 1.936 mm (with m = 11, n = 12) as shown in Fig. 3. It is clear that the selected wave plate thickness gives rise to both high transmittances and large isolations over 60 dB for λ_1 and λ_2 lights simultaneously, which is much higher than the typical ∼20–30 dB isolation of commercial products.

When an l = 1.936 mm-thick Quartz crystal is employed, the transmission spectra of this bidirectional isolator are shown in Fig. 4. The solid line denotes the forward direction while the dashed line is for the backward direction. In the forward, the light (λ_1 = 1.49 μm) may pass with low loss while (λ_2 = 1.31 μm) light is isolated. In the backward, the status is reversed, λ_1 light is blocked and the λ_2 signal travels freely. From the figure, the corresponding insertion loss is around 0.044 dB without consideration of the Fresnel reflection. This is actually the extra loss to realize the bidirectional isolation function. To our knowledge, the loss of a practical isolator mainly consists of propagation loss and coupling loss, which might be much larger than the obtained 0.044 dB. It means our design is feasible. The final loss should be still around the same level as that of traditional isolators.

If the light signal deviate from working wavelength, the optical isolation will drop rapidly. Therefore, it is hard to achieve the highest isolation. The wavelength bandwidth is a more valuable parameter based on tolerance analysis. According to Eq. (4), the transmittances of any wavelength are,

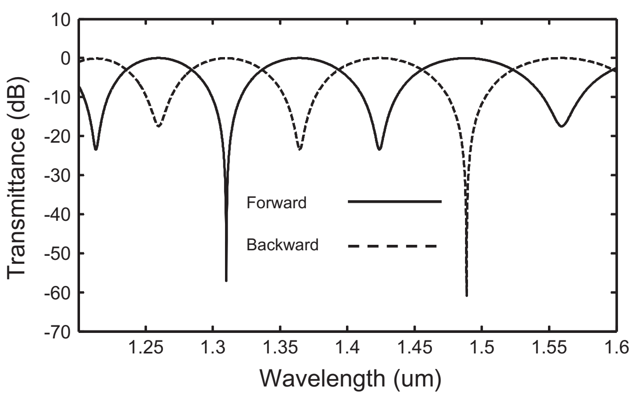

Fig. 4. Output spectra of a bidirectional isolator. The solid line denotes the forward direction, and the dashed line is for the backward direction.

$$T_{forward} = \cos^2(g-\phi)\cos^2(\Gamma/2) + \cos^2(g-\phi-2\alpha)\sin^2(\Gamma/2),$$
$$T_{backward} = \cos^2(g+\phi)\cos^2(\Gamma/2) + \cos^2(g+\phi+2\alpha)\sin^2(\Gamma/2). \tag{14}$$

In the forward direction, if the signal wavelength has a small deviation ($\delta\lambda$) from λ_2, scilicet $\lambda = \lambda_2 + \delta\lambda$, the transmittance near λ_2 is,

$$T_{forward} \approx (\delta\lambda)^2(\Gamma_2^2/4 + g_2^2)/\lambda_2^2. \tag{15}$$

The situation in the opposite direction is similar. If the wavelength has a slight deviation ($\delta\lambda$) from λ_1, the transmittance near λ_1 is,

$$T_{backward} \approx (\delta\lambda)^2(\Gamma_1^2/4 + g_1^2)/\lambda_1^2. \tag{16}$$

From Eqs. (14) and (15), the drop of optical isolation is proportional to the square of deviated wavelength ($\delta\lambda$). The tolerance coefficient η thus could be obtained as,

$$\eta = (\Gamma^2/4 + g^2)/\lambda^2. \tag{17}$$

Smaller η results in more slightly transmittance change, corresponding to wider bandwidth. Because the phase retardation Γ is proportional to wave plate thickness, thinner wave plate is more desired for a bidirectional isolator. For our current design, the obtained bandwidths at 20 dB and 30 dB isolation are 7 nm and 2 nm, respectively, for both λ_1 and λ_2 lights.

In our design above, the wave plate is a fixed Quartz crystal so that its thickness should be well-selected. To overcome this difficulty, it could be replaced by a homogeneous alignment LC cell with tunable phase-retardation. We can adjust the LC driving voltage to critically tune the operation wavelength. An extreme case would be swapping the isolation directions for (λ_1) and (λ_2) signals, i.e., it is tuned to be a full wave plate of (λ_2) and half wave plate of (λ_1). This tunable isolator may have some more unique applications. In above, we only studied the dual-wavelength (1.49 μm, 1.31 μm) case, which is relatively simple. If more wavelengths are induced or wider bandwidth is required, maybe multiple wave plate stacking will be used. Moreover, our proposed design is still relatively bulky. To obtain a more miniature device, a higher birefringent wave plate could be used. Based on our design principle, a more compact micro-optical isolator might be expected.

3. Conclusions

In summary, we proposed a bidirectional optical isolator with wavelength selective function. Being different from traditional isolators, an additional specially-designed wave plate is sandwiched by a polarizer and a Faraday rotator. As an example, a (1.49 μm, 1.31 μm) isolator was designed by using direct analysis and Jones Matrix method. The insertion loss, maximum isolation and wavelength bandwidth all meet the current telecom requirements. Some approaches to improve isolator performances are also discussed. We believe this device should be useful in the new generation of optical communications or sensing systems.

Acknowledgments

This work is sponsored by 973 program with Contract Nos. 2011CBA00200 and 2010CB327800, NSFC program under Contract Nos. 10874080 and 60977039. We acknowledge the support from China New Century Excellent Talents program and Specialized Research Fund for the Doctoral Program of Higher Education.

References

[1] T. Amemiya, T. Tanemura, Y. Nakano, Nonreciprocal polarization converter consisting of asymmetric waveguide with magneto-optic cladding: theory and Simulation, IEEE J. Quant. Electron. 45 (2009) 769–776.
[2] R.Y. Chen, D.J. Tao, H.F. Zhou, Y.L. Hao, J.Y. Yang, M.H. Wang, X.Q. Jiang, Asymmetric multimode interference isolator based on nonreciprocal phase shift, Opt. Commun. 282 (2009) 862–866.
[3] X.H. Ye, J.P. Li, X.J. Huang, M. Zhang, P.D. Ye, A bulk optical isolator with high optical performance, Opt. Commun. 275 (2007) 65–70.
[4] K. Shiraishi, T. Yanagi, Y. Aizawa, S. Kawakami, Fiber-embedded in-line isolator, IEEE J. Lightw. Technol. 9 (1991) 430–435.
[5] F. Effenberger, T.S. El-Bawab, Passive optical networks (PONs): past, present, and future, Opt. Switch. Network. 6 (2009) 143–150.
[6] Z.F. Yu, S.H. Fan, Complete optical isolation created by indirect interband photonic transitions, Nat. Photon. 3 (2009) 91–94.
[7] Q. Wang, F. Xu, Z.Y. Yu, X.S. Qian, X.K. Hu, Y.Q. Lu, H.T. Wang, A bidirectional tunable optical diode based on periodically poled $LiNbO_3$, Opt. Exp. 18 (2010) 7340–7346.
[8] H.F. Zhou, X.Q. Jiang, J.Y. Yang, Q. Zhou, T.B. Yu, M.H. Wang, Wavelength-selective optical waveguide isolator based on nonreciprocal ring-coupled Mach–Zehnder interferometer, IEEE J. Lightw. Technol. 26 (2008) 3166–3172.
[9] M.S. Lee, I.K. Hwang, B.Y. Kim, Bidirectional wavelength-selective optical isolator, Electron. Lett. 37 (2001) 910–912.
[10] K. Xie, H.M. Jiang, W.Y. Zeng, G.J. Wen, H.J. Yang, A.D. Boardman, M. Xie, Elimination of phase-matching requirement for optical waveguide isolator, Opt. Commun. 282 (2009) 3883–3888.
[11] M. Shirasaki, K. Asama, Compact optical isolator for fibers using birefringent wedges, Appl. Opt. 21 (1982) 4296–4299.
[12] Y. Shoji, H. I-Wei, R.M. Osgood, T. Mizumoto, Polarization-independent magneto-optical waveguide isolator using TM-mode non-reciprocal phase shift, IEEE J. Lightw. Technol. 25 (2007) 3108–3113.
[13] Y.Q. Lu, C. Wang, S.T. Wu, A liquid crystal-based fourier optical spectrum analyzer, IEEE Photon. Technol. Lett. 16 (2004) 861–863.
[14] C.S. Kang, H.J. Kong, Liquid crystal linear polarizers for Faraday isolator in a high-power laser system, IEEE Photon. Technol. Lett. 4 (1992) 1038–1040.
[15] Y. Shoji, T. Mizumoto, Wideband design of nonreciprocal phase shift magneto-optical isolators using phase adjustment in Mach–Zehnder interferometers, Appl. Opt. 45 (2006) 7144–7150.